Synthesis and characterization of ordered mesoporous silicas for the immobilization of formate dehydrogenase (FDH)

Synthesis and characterization of ordered mesoporous silicas for the immobilization of formate dehydrogenase (FDH)

Giuseppe Pietricola[1], Tonia Tommasi[1], Melodj Dosa[1], Enrico Camelin[1], Emanuele Berruto[1], Carminna Ottone[2**], Debora Fino[1], Valentina Cauda[1], Marco Piumetti[1*]

[1]Department of Applied Science and Technology,
Corso Duca degli Abruzzi 24, Politecnico di Torino, I-10129, Turin (Italy).
**) marco.piumetti@polito.it*

[2]Escuela de Ingeniería Bioquímica, Pontificia Universidad Católica de Valparaíso, Av. Brasil 2085, Valparaíso, Chile
***) carminna.ottone@pucv.cl*

Abstract

This work studied the influence of the pore size and morphology of the mesoporous silica as support for formate dehydrogenase (FDH), the first enzyme of a multi-enzymatic cascade system to produce methanol, which catalyzes the reduction of carbon dioxide to formic acid. Specifically, a set of mesoporous silicas was modified with glyoxyl groups to immobilize covalently the FDH obtained from *Candida boidinii*. Three types of mesoporous silicas with different textural properties were synthesized and used as supports: i) SBA-15 (D_P = 4 nm); ii) MCF with 0.5 wt.% mesitylene/pluronic ratio (D_P = 20 nm) and iii) MCF with 0.75 wt.% mesitylene/pluronic ratio (D_P = 25 nm). As a whole, the immobilized FDH on $MCF_{0.75}$ exhibited higher thermal stability than the free enzyme, with 75% of residual activity after 24 hours at 50 °C. FDH/$MCF_{0.5}$ exhibited the best immobilization yields: 69.4% of the enzyme supplied was covalently bound to the support. Interestingly, the specific activity increased as a function of the pore size of support and then the FDH/$MCF_{0.75}$ exhibited the highest specific activity (namely, 1.05 UI/$g_{MCF0.75}$) with an immobilization yield of 52.1%. Furthermore, it was noted that the immobilization yield and the specific activity of the FDH/$MCF_{0.75}$ varied as a function of the supported enzyme: as the enzyme loading increased the immobilization yield decreased while

the specific activity increased. Finally, the reuse test has been carried out, and a residual activity greater than 70% was found after five cycles of reaction.

Graphical abstract

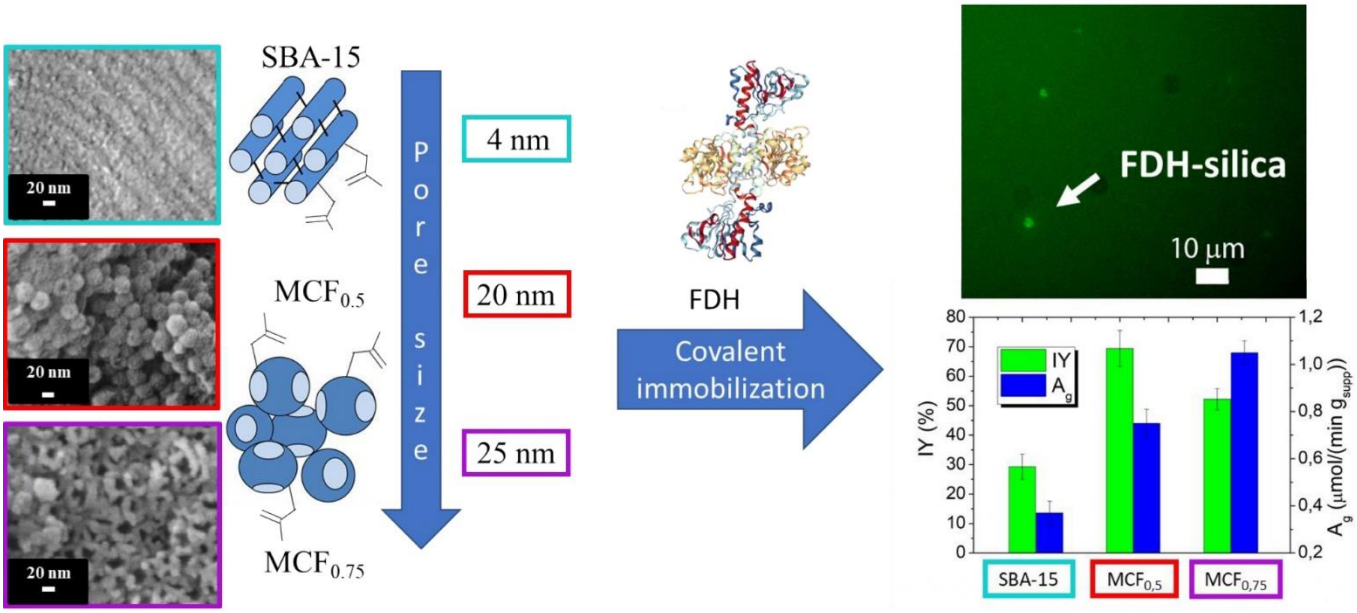

Keywords

Formate dehydrogenase; Ordered mesoporous silicas; Covalent immobilization; Glyoxyl functionalization; Fluorescence microscopy.

1. Introduction

The IPCC (International Panel on Climate Change) established that the increasing concentration of atmospheric carbon dioxide (CO_2) is the principal cause of Global Warming [1]. Therefore, this issue has recently received a great deal of attention and new approaches have been developed, such as biological CO_2 conversion through enzymatic routes [2–4]. These new biotechnological approaches have some attractive advantages compared to the traditional inorganic ways of reducing CO_2 to chemicals, such as milder reaction conditions, higher yields and selectivity, and eco-friendliness [3,5]. In particular, the enzymatic process of CO_2 reduction to methanol exploiting enzyme-catalyzed cascade reactions with different dehydrogenases (Figure 1) appears very promising, with a methanol yield (referring to the initial amount of NADH) which may be greater than 95% [6,7]. This bioprocess is formed by three reactions in series: i) reduction of CO_2 to formic acid by formate dehydrogenase (FDH), ii) reduction of formic acid to formaldehyde by formaldehyde dehydrogenase ($F_{ald}DH$) and iii) reduction of formaldehyde to methanol by alcohol dehydrogenase (ADH). The cofactor nicotinamide adenine dinucleotide (NADH) acts as the electron donor for each reaction catalyzed by the dehydrogenases [8,9]. High concentrations of NADH cofactor are necessary to carry out the reactions of interest. NADH regeneration on a laboratory scale can be performed with different techniques, such as enzymatic or chemical regeneration [6,10,11]. Another promising strategy is the electrochemical regeneration, which may allow to work in a semi-continuous way [12] and achieving active NADH regeneration yields greater than 75% [13]. Moreover, this technique also permits to simultaneously carry out the reaction of interest and the cofactor's regeneration [14].

Each enzyme of the series can be extracted from more than one organism, and this choice could allow higher values of specific activity [15]. For instance, FDH enzymes from *C. boidinii, Thiobacillus sp. and Paracoccus sp*. have been studied for the CO_2 reduction reaction, showing different performances, both in the reduction of CO_2 and in the oxidation of formic acid [2]. Similarly, the enzyme of interest in this work is the FDH enzyme. To the best of our knowledge, the most active enzyme in the CO_2 reduction reaction is the one extracted from *Thiobacillus sp* [2]. However, it is more common to find studies with that extracted from *Candida boidinii* due to its large presence on the market. Several works showed that the three dehydrogenases' confinement in a solid porous matrix increases the yield of the total reaction compared to a

homogeneous system. This is due to an overall local increase in the concentration of the reactants within the support's pores where the enzymes are located [8,16]. Moreover, immobilization is pivotal for future industrial developments because it increases the enzyme's stability [17]. Therefore, it is essential to find out the optimal support for the immobilization of the three enzymes (FDH, F_{ald}DH, ADH) to enhance the reduction of CO_2 and enable maximum enzyme reuse. Different techniques and materials have been applied for the immobilization of these enzymes (both co-immobilized and separately immobilized): encapsulation in silica sol-gel matrix [8], encapsulation in an alginate-silica matrix [7], entrapment in PVA hydrogel or alginate gel [18], hybrid microcapsules with different immobilization techniques for each enzyme [19] and many others. As a study strategy, each enzyme can be immobilized independently of the others to optimize each immobilization condition.

In this scenario, a promising immobilization technique on hierarchical porous materials is the multipoint covalent attachment, which has led to great results with a broad group of enzymes [20–22]. In order to enable the formation of covalent bonds between the enzyme and the support, the latter is previously activated with surface aldehyde groups that are highly reactive with enzyme's non-ionized amine groups. Such aldehyde-activated supports are commonly named glyoxyl supports. Hence, this method guarantees strong enzyme-support interactions, which prevent enzyme leaching and stabilize the biocatalyst (support with enzyme) at higher temperatures.

The support choice is another fundamental aspect for the immobilization process: it should consider some of its essential characteristics, such as a high surface to volume ratio, compatibility and insolubility in the reaction medium, high mechanical and chemical stability [17]. Mesoporous silicas (e.g. SBA-15, MCM-41, MCM-48 and MCF) have been used for the immobilization of different enzymes with successful results [23,24],with their applications as supports also for FDH, FalDH and ADH [9,25–27]. These materials can be synthesized in different ways resulting in diverse pore structures (e.g. hexagonal, cubic, foam-like) with tunable pore sizes (from 2 to 50 nm) [9,28]. The structure, the dimension and the accessibility of the support's pores are key parameters for the immobilization of an enzyme. Therefore, there is an urgent need to evaluate which specific supports are optimal for the immobilization of each specific enzyme. Zezzi do Valle Gomes and Palmqvist [9] and Nabavi Zadeh and colleagues [27], used mesoporous silica (MCF-type material) for the immobilization of F_{ald}DH and both F_{ald}DH and FDH, respectively. They obtained successful results with MCF modified with

functional groups (octyl, mercaptopropyl and chloromethyl) using physical adsorption to immobilize the enzymes. This immobilization strategy has often given good results with lipases since they display a high number of non-polar amino acid residues [29]. On the other hand, enzymes such as FDH, having fewer apolar groups on the surface, would form a weaker bond with the support and be desorbed in solution.

As mentioned before, a crucial problem in biocatalysis is the stability of enzymes. Thus, the development of an immobilization process that increases the enzymatic stability and ensures the use of the biocatalyst for more reaction cycles is essential. Furthermore, the support must have a low production cost. To this aim, three different low-cost mesoporous siliceous materials were synthesized and used as support for FDH immobilization. In order to obtain a good increase in thermal stability and a high number of reuse cycles, these supports were functionalized with glyoxyl groups for the covalent immobilization of the FDH enzyme. Glyoxyl modification on commercial mesoporous silica has already been used to immobilize FDH from *Candida methylica* [30]. To the best of authors' knowledge, synthesized silica functionalized with glyoxyl groups has never been used to immobilize FDH from *Candida boidinii*. Furthermore, the effect of the pore size of the support on the activity of the FDH enzyme has never been evaluated. For this purpose, three different synthesized mesoporous silica (SBA-15, $MCF_{0.5}$ and $MCF_{0.75}$) were analyzed. So, the ability to control and tune the average pore diameter of the support allowed the study of the influence of the pore size and morphology of the mesoporous silicas on immobilization yield and specific activity of FDH. All the synthesized materials were characterized by complementary techniques such as X-ray Diffraction (XRD), Field Emission Scanning Electron Microscopy (FESEM) and N_2 physisorption at -196 °C.

The thermal stability was measured for the most promising porous support, namely the $MCF_{0.75}$. The variation of the immobilization yield and the specific activity as a function of the enzymatic load were evaluated on this support. Furthermore, optical fluorescence microscopy allowed to verify the presence of the immobilized enzyme directly. The variation of specific activity as a function of pH and temperature was also evaluated. Finally, a reuse test was carried out to assess the residual activity of the enzyme.

The use of these tailor-made materials and the modification with glyoxyl groups could be replicated with other FDHs exhibiting a greater activity towards CO_2 reduction. Another fascinating perspective is the implementation of the co-immobilization of the three enzymes to produce methanol from CO_2. Lastly, these materials are good candidates for the immobilization

of any other type of enzyme different in size and shape from *Candida boidinii* FDH since their synthesis strategies allows the fine control of their pores size.

2. Materials and methods

2.1 Materials

(3-Glycidyloxypropyl)trimethoxysilane (GPTMS, ≥98%), sulfuric acid (≥98%), sodium borohydride (≥98%), hydrochloric acid (37% wt.), poly(ethylene glycol)-block-poly(propylene glycol)-block-poly(ethylene glycol) (Pluronic P-123), tetraethylorthosilicate (TEOS, 99% wt.), 1,3,5-trimethylbenzene (mesitylene, 98% wt.), sodium metaperiodate, glycerol and sodium formate were supplied from Merck. Formate Dehydrogenase (FDH) from *Candida boidinii* was purchased from Megazyme. NAD^+ (99.6%) was supplied from PanReach AppliChem and NADH (97.1%) from Acros Organics.

2.2 Methods

2.2.1 Synthesis of the supports

SBA-15 was synthesized according to the procedure reported in Ref. [31]. Briefly, 30 mL of deionized water and 160 mL of 2 M HCl were mixed into a beaker. Then, 4 g of P-123 (templating agent) were softened into the solution and mixed under vigorous stirring at room temperature (r.t) for 5 h in order to create a homogeneous solution. Next, 8.5 g of TEOS were drop-wised into the solution to guarantee a proper dispersion of the components during the mixing phase. After that, the solution was stirred at r.t. for 24 h. Then, the suspension was transferred into a Teflon autoclave and aged at 100 °C for other 24 h. Finally, the precipitated was filtered by a vacuum pump, washed with deionized water, dried overnight at 100 °C and calcined at 550 °C (heating rate 10 °C min^{-1}) for 5 h.

The MCF support was synthesized by modifying a literature procedure [31,32] in which P-123 is the templating agent and mesitylene is the organic swelling agent, with mesitylene-to-P-123 ratio 0.5 or 0.75 (wt./wt.). In a typical synthesis, 4 g of Pluronic P-123 were softened into a

beaker with 150 mL of HCl (1.6 M) and mixed at 40 °C for 1 h. Then, 2 or 3 mL of mesitylene were drop-wised into solution (if the final mesytilene-to-P-123 ratio were respectively 0.5 or 0.75) [28,33,34].

After that, 8.5 g of TEOS were added by drop-wising into the previous solution and maintained under constant stirring at 40 °C for 24 h. Then, the suspension was put inside a Teflon autoclave for a hydrothermal treatment at 100 °C for 24 h in order to increase both window size and the cell of the foam. Finally, the suspension was filtered by vacuum pump, washed with deionized water and dried overnight at 100 °C. Subsequently, the MCF obtained was calcined at 500 °C for 6 h, with a heating rate of 10 °C min^{-1} [33–35].

Two MCF samples were synthesized and herein were labelled as "$MCF_{0.5}$" and "$MCF_{0.75}$" in which the subscript indicates the mesytilene-to-P-123 ratio.

2.2.2 Structural and textural characterization of the supports

Powder X-ray diffractograms of the supports were recorded on an X'Pert Philips PW3040 diffractometer using Cu Kα radiation ($2\theta < 2°$; step = 0.014° 2θ; time per step = 0.2 s). The diffraction peaks were indexed according to the Powder Data File database (PDF 2000, International Centre of Diffraction Data, Pennsylvania).

The textural properties of the supports were investigated as follows: the BET (Brunauer–Emmett–Teller) specific surface area (S_{BET}) was measured by means of N_2 physisorption isotherms at −196 °C on 70 mg sample previously outgassed at 200 °C for 2 h to remove molecular water and other atmospheric contaminants (Micrometrics Tristar II, USA instrument); the total pore volume (V_p) was calculated at $P/P_0 = 0.97$; the micropore volume (V_{micro}) was evaluated by the t-plot method; the average pore diameter (D_p) was calculated by either applying the Barrett–Joyner–Halenda (BJH) algorithm to the isotherm desorption branch (SBA-15) or according to a modified Broekhoff de Boer (BdB) method using Hill's approximation for the adsorbed layer thickness (MCF materials) [36].

Sample morphology was analyzed through FESEM microscopy (Zeiss MERLIN, Gemini-II column).

2.2.3 Functionalization of supports

Covalent binding of the enzymes on the support was conducted with a functionalization step to create glyoxyl groups on the support using the GPTMS reagent [20,37]. The protocol was modified from the literature [20]. First, epoxy groups were created, putting the support in contact with GPTMS (1% v/v in toluene) at 105 °C for 5 h. Subsequently, the epoxy ring was opened, carrying out a hydrolysis reaction to generate diol groups with a 0.1 M sulfuric acid solution for 2 h at 85 °C [38]. Finally, oxidation of the diol groups to glyoxyl occurred using a 0.1 M sodium periodate solution for 2 h at r.t. [20]. The amount of glyoxyl groups generated was obtained by back titration, as described by Guisan [39]. The content of glyoxyl groups on the three functionalized support was about 250 μmol/g_{supp}. The three reaction steps were carried out under strong stirring.

2.2.4 Enzymatic activity assay

Activity tests were performed using a Jasco V-730 UV-visible spectrophotometer. A cuvette containing 2.3 mL of phosphate buffer at pH 7.5 (0.1 M), 0.5 mL of sodium formate (0.3 M) and 0.1 mL of NAD^+ (50 mM) was used. To test the activity of the free enzyme, 0.05 mL of FDH dilute solution (1:100 from the commercial solution: 25 ± 1 $mg_{protein}$/ml) were added. Instead, in the case of the immobilized enzyme, 10 mg of support were added. The change in absorbance at 340 nm was used to monitor the NADH formation. The activity is expressed in IU (international unit) and corresponds to the amount of enzyme necessary to produce one μmol per minute of NADH at pH 7.5 and 30 °C [40]. The specific activity (A) is the activity referred to one mg of protein in solution in the case of the free enzyme. In the case of immobilized FDH, the specific activity (A) can be referred to one g of biocatalyst ($A_{g.\ supp.}$) or one mg of protein immobilized on the support ($A_{mg.\ imm.\ prot.}$).

The size of the enzyme was calculated by approximating its shape to a sphere, and the minimum diameter that can contain the enzyme was calculated using equation (1) [41]:

$$R_{min} = 0.066 \cdot M^{\frac{1}{3}} \quad (1)$$

where M is enzyme weight in Da and R_{min} is enzyme radius in nm.

2.2.5 Enzyme immobilization

The functionalized support and the enzyme FDH were put in contact in a 0.1 M phosphate buffer solution at pH 10.05 with 15% v/v glycerol at T = 4 °C. As reported in the literature, immobilization was carried out under mild agitation to avoid denaturation of the enzyme [42]. An enzymatic load of q = 2 mg_{prot}/g_{supp} in the immobilization solution was used.
Samples of supernatants were taken in a time-course analysis to perform the activity assay and the quantification of the protein with the Bradford assay [43]. Simultaneously, activity tests were also carried out on the blank (solution of FDH in the same condition of the immobilization solution, but without support) to control the stability of the free enzyme in the conditions of immobilization. After 1 h, sodium borohydride (0.5 mg/mL) was added in order to stabilize and create a covalent bond between enzyme and support. To quantify the immobilization yield (IY), the concentration of protein in solution was measured, through the Bradford assay [43], at the beginning ($C_{prot,t0}$) and the end ($C_{prot,tf}$) of the process. Thus, IY is expressed in equation (2) [17]:

$$IY\ (\%) = \frac{C_{prot,t_0} - C_{prot,t_f}}{C_{prot,t_0}} \cdot 100 \qquad (2)$$

The specific activity can be expressed as a percentage in the form of the retained activity (R_{act}) [44] by equation (3) as:

$$R_{act}\ (\%) = \frac{A_{g\ supp.}}{q \cdot A_{FE,t_0}} \cdot 100 = \frac{A_{g\ supp.}}{C_{act}} \cdot 100 \qquad (3)$$

where $A_{g.\ supp.}$ is the specific activity of the immobilized enzyme, q is the enzymatic load provided, $A_{FE,t0}$ is the specific activity of the free enzyme at the beginning of the immobilization.

2.2.6 Thermal stability

The free and the immobilized enzyme were incubated in a bath at T = 50 °C. The activity test was carried out at different times to see the decrease in activity over time. The residual activity

(A) is expressed as a percentage of starting activity (A_0). A first-order deactivation model with no residual activity was used to describe the deactivation of the free and the immobilized enzyme [17], expressed in equation (4) as:

$$A = A_0 \cdot e^{-k_D \cdot t} \qquad (4)$$

where k_D represents the deactivation constant (h^{-1}) and t the time (h). It was, therefore, possible to obtain the half-life ($t_{1/2}$) and finally the stabilization factor (F_S), expressed in the equation (5):

$$F_S = \frac{t_{\frac{1}{2},imm.enz.}}{t_{\frac{1}{2},sol.enz.}} \qquad (5)$$

2.2.7 Fluorescence labelling and microscopy

Fluorescent labelling was performed to visualize the enzyme immobilized on the mesoporous silica sample $MCF_{0.75}$. Operatively, 1 mg of $MCF_{0.75}$ sample was dispersed in 1 mL of a 100 mM sodium bicarbonate buffer solution (pH 9.5) at room temperature. A solution of 1 mg/ml fluorescein isothiocyanate (FITC, $\lambda_{excitation}$=488 nm, $\lambda_{emission}$= 525nm) in dimethylsulfoxide (DMSO) was then added to obtain a molar ratio of 20:1 FITC-to- enzyme immobilized in the silica sample. The solution was then orbitally shaken at 300 rpm at r.t. for 1 hour. Reasonably, the isothiocyanate groups of FITC covalently bound the amine terminations present in the FDH enzymes. As a control experiment, 1 mg of $MCF_{0.75}$ mesoporous silica without enzyme was also combined with the same amount of dye. In the end, both samples were washed three times, centrifuging the silica solution at 1000 rcf for 5 minutes in a benchtop centrifuge and redispersed in 1 mL of the sodium carbonate buffer. To successfully remove the unbound or only physically retained FITC from the silica, 1 mL of fresh bicarbonate solution was added to each sample after the last washing step and left overnight under orbital shaking at r.t.. Afterwards, both silica samples were centrifuged and washed twice as described above and finally dispersed in 1 mL of fresh buffer each. The samples were then analyzed through fluorescence microscopy. A 10-µl drop of each sample solution was deposited on a glass microscope slide, covered with a cover glass slip (0.17-mm thick; VWR) and analyzed with a

wide-field fluorescence-inverted microscope (Eclipse Ti-E, Nikon, Tokyo, Japan), equipped with a super bright wide-spectrum source (Shutter Lambda XL), a high-resolution camera (Zyla 4.2 Plus, 4098 × 3264 pixels, Andor Technology, Belfast, UK) using an immersion oil 60× objective (Apo 1.40, Nikon). The NIS-Element software (NIS-Elements AR 4.5, Nikon) was used to acquire the picture. Images were acquired in the brightfield channel and in the green channel, modifying the protocol present in the literature [45].

2.2.8 Variation of enzymatic activity with pH and temperature

The dependence of the enzymatic activity on temperature and pH was evaluated by carrying out the activity test, as described in section 2.2.4. The tests were carried out changing the buffer pH and the incubation temperature. In particular, to evaluate the influence of temperature, the pH was kept fixed at 7.5, and the activity test was conducted at 30 °C, 40 °C, 50 °C, 60 °C. To evaluate the influence of pH, at a fixed temperature of 30 °C, the following buffers were used: a 0.1 M phosphate buffer at pH 6, 7, 7.5 and 8, and a 0.1 M carbonate buffer for the solution at pH 9 and 10. The values obtained were expressed as a percentage of the maximum value for each series of experiments.

2.2.9 CO_2 reduction

The reaction was carried out at r.t. under shaking (300 rpm) in 30 mL of 0.1 M phosphate buffer at pH 7 in a sealed glass bottle, pre-saturated with CO_2, in presence of NADH 10 mM and 1.0 g of FDH/$MCF_{0.75}$. The reaction conditions used are the same as those used in our previous work [22]. Formic acid was analyzed in a Shimadzu Prominence HPLC equipped with a refractive index detector using a Rezex ROA-Organic acid H^+ (8%) column (300 mm × 7.8 mm). Samples were eluted with H_2SO_4 5 mM at a flow rate of 0.6 mL/min, and the column temperature was fixed at 50 °C. Formic acid (HPLC grade) was used to determine the retention time and to check the linear range of the measurements.

2.2.10 Reusability of the immobilized FDH

Several closed batch reactions, carried out at 300 rpm, were performed as described in section 2.2.10 to study the reuse of the immobilized enzyme. After each batch, the immobilized enzyme was filtered and washed with distilled water. Subsequently, activity was measured at pH 7.5 and T = 30 °C, as described in Section 2.2.4. Activity after each reaction was expressed as a percentage of the initial value.

2.2.11 Statistical analysis

Immobilization yields, specific activities, deactivation constants and half-life times were analyzed by one-way ANOVA (analysis of variance) with a Tukey's post hoc test ($P \leq 0.05$). ANOVA was run after the assessment of its fundamental assumptions, namely the normality of distributions (Shapiro-Wilk test, p-value > 0.05) and the homogeneity of the variances of the residuals (Levene's test with P(>F) > 0.05). The statistical software R (version 4.0.3 - “Bunny-Wunnies Freak Out”) was used for all statistical analysis.

3. Results and discussions

3.1 Characterization of supports

3.1.1 X-ray Diffraction (XRD) and N_2 physisorption at -196 °C

Figure 2 shows the XRD spectrum of the SBA-15 sample at low 2θ angles. As a whole, the XRD pattern of the synthesized SBA-15 is in agreement with the literature [46–49].
Indeed, the SBA-15 exhibits the (100), (110) and (200) reflection peaks attributed to the typical hexagonal space group (*p6mm*) symmetry characteristic of mesoporous SBA-15 [32].
Thanks to the regular structure of SBA-15 it is possible to evaluate interesting cell parameters: the inter-reticular distance (d_0) the cell parameter (a_0) and the wall thickness (δ) (scheme in Figure 2). Specifically, the d_0 can be evaluated by equation (6):

$$d_0 = \frac{\lambda}{2\sin(\theta)} \qquad (6)$$

where λ is the $K_{\alpha 1}$ of Cu XRD source (1.540598 Å) and θ is the half-angle of (100) peak position (0.955/2= 0.4775°). Thus, d_0 is 9.2 nm. The a_0 can be evaluated by equation (7):

$$a_0 = \frac{2d_0}{\sqrt{3}} \qquad (7)$$

The a_0 is 10.7 nm. The wall thickness (δ) is evaluated by equation (8):

$$\delta = a_0 - D_{BJH} \qquad (8)$$

where D_{BJH} (= 4 nm) is the pore diameter evaluated by the BJH-method (see Table 1). Thus, the wall thickness δ is 6.7.

Conversely, the XRD patterns for the MCF-type supports do not exhibit any diffraction peaks because this material has not a long-range order structure (spectra not reported for the sake of brevity).

In Table 1, the main textural properties derived from the N_2 physisorption at -196 °C are reported. As a whole, SBA-15 exhibits the higher surface area (674 $m^2\ g^{-1}$) in the set of the prepared materials ($MCF_{0.5}$ = 573 $m^2\ g^{-1}$, $MCF_{0.75}$ = 600 $m^2\ g^{-1}$). Moreover, the higher the mesitylene-to-P-123 ratio, the better the textural properties for the MCF, in agreement with previous studies [31,32,50].

Figure 3 shows the N_2 sorption isotherms for the prepared materials. As a whole, they display type IV profiles typical of mesostructured materials [32,51–53].

SBA-15 (curve a) shows H1 hysteresis loop, which is characteristic for this material [48,54]. The increase in the p/p_0 range 0.4-0.6 is due to the capillarity condensation phenomenon in the mesoporous channels. Also, the presence of larger pores (about 4 nm) is in accordance with the shift at a higher relative pressure (p/p_0 ~ 0.6) that corresponds to the N_2 primary condensation in the mesopores [51,55].

Interestingly, the MCF supports (curves b and c) exhibit type H1 hysteresis loops shifted to higher relative pressures, thus indicating the presence of larger pores, known as “closed cells” (average diameter 20-25 nm), connected each other with small windows (about 14 nm) [46]. Moreover, the $MCF_{0.75}$ hysteresis loop represents a higher area comparing with that for $MCF_{0.5}$. Our previous studies indicated that the pore sizes of $MCF_{0.5}$ and $MCF_{0.75}$ evaluated by the BdB-FHH method correspond to 20 and 25 nm, respectively [31,32].

3.1.2 FESEM analysis

The typical worm-like array of SBA-15-type material is shown in Figure 4a, along with its magnification. In the magnification, it is possible to observe the parallel channels peculiar of this material [31].
Moreover, the MCF supports exhibit the typical spongy-like structure with cavities (Figures 4b and 4c). In particular, when the mesitylene/P-123 ratio is higher (0.75), the cavities are larger (magnification in Figure 4c) than the ones obtained with the lower mesitylene/P-123 ratio (magnification in Figure 4b). These morphological features confirm the textural results achieved with N_2 physisorption (Table 1) and are in fair agreement with previous studies [31,32,50].

3.2 Characterization and testing of the free and immobilized formate dehydrogenase

The specific activity of the commercial enzyme solution was 5.2 ± 0.1 IU/mg_{prot}. The Bradford test was carried out to obtain the quantity of protein inside the commercial solution of FDH, which turned out to be equal to 25 mg/ml.
It is possible to approximate the enzyme shape to a sphere in order to calculate an indicative size of the enzyme. The molecular weight of the enzyme (M) is equal to 74000 Da [56]. Using the equation (1), a diameter equal to D = 5.54 nm is obtained.

3.2.1 Comparison between different support materials

In the immobilization solution, all the supports were put in contact with an enzymatic load q = 2 mg_{prot}/g_{supp}. The duration of the immobilization process was the same for all tests, namely one hour. In this way, it was possible to compare the different supports, having different textural and structural properties. As a result, the immobilization yields varied significantly with the (average) pore size of the particles (Table 2). Using the SBA-15, (average pore diameter of about 4 nm) the immobilization yields were lower than in other cases since the enzyme has a diameter of about 6 nm. Indeed, it could only bind the support external surface, without diffusing inside the pores. With this support, the specific activity per mg of immobilized protein is higher than with $MCF_{0.5}$. In fact, when the enzyme was immobilized only on the external surface of the channels,

it was less sensitive to limitations due to mass transfer. After exceeding the enzyme's diameter (6 nm), IY decreases along with the increase of the mean pore diameter.

The larger the pores, the higher the activity values as the reagents and the products can diffuse more easily inside and outside the pores, respectively. In particular, as reported in Table 2, the differences in activity (both per mg of enzyme and per g of support) are significant. Therefore, $MCF_{0.75}$ was the support allowing higher enzyme activity. Considering that the FDH/$MCF_{0.75}$ showed the best specific activity values related to the immobilized enzyme, subsequent tests were carried out only with this support. The immobilization yield results with $MCF_{0.5}$ and $MCF_{0.75}$ are in line with other ones reported in the literature, obtained with supports modified with glyoxyl groups. For example, immobilization yields ranging from 50 to 100% with glyoxyl agarose [40,42], from 50% to 76% with glyoxyl natural zeolite [22] and 75% with glyoxyl silica [30] are obtained.

The retained activity, defined according to equation (3), was 14% for $MCF_{0.75}$ and 10% for $MCF_{0.5}$ are obtained. These values are comparable to those of other works where the expressed activity ranged from 5% to 90% and from 14% to 40% with FDH from *Candida boidinii* respectively immobilized on glyoxyl agarose [42] and glyoxyl natural zeolite [22]. Conversely, both the specific activity and the immobilization yield obtained with FDH/SBA-15 are lower and probably attributable to the reduced size of the pores of this support, thus not suitable for the immobilization of the FDH enzyme.

3.2.2 Fluorescence microscopy imaging of the enzyme immobilization

In order to verify the enzyme presence on the immobilized silica support, a clear and unique proof can be provided by optical fluorescence microscopy, after labelling the enzyme with a fluorescent dye. For this experiment, only the mesoporous silica $MCF_{0.75}$ showing the highest FDH specific activity was used, as reported in Table 2.

As previously described in the Materials and Method section, the biocatalyst was combined with a green-emitting fluorescent dye, FITC, which should specifically bind the enzyme's amino groups. Figure 5 exhibits FDH/$MCF_{0.75}$ after FITC labelling; the sample shows a bright fluorescence emission in the green channel (Figure 5b) which colocalizes with the silica particles position in the brightfield (Figure 5a). The negative control, the same silica $MCF_{0.75}$

without FDH enzyme, does not show any green fluorescence emission (Figures 5c and 5d). This observation confirms that the enzyme FDH is properly immobilized on the $MCF_{0.75}$ support.

3.2.3 Evaluation of the enzyme loading

In the case of $MCF_{0.75}$ support, the yield of the immobilization and the specific activity varied along with the enzymatic load supplied. Indeed, Figure 6a lends support to this thesis, showing that the yield of immobilization decreases while the amount of immobilized enzyme increases, with a constant immobilization time of 1 h. Although the specific activity per gram of the biocatalysts made with the different supports varies, the specific activity per mg of immobilized enzyme is approximately the same in the 5 cases analyzed (1.1 ± 0.1 IU/mg_{enz}). The specific activity per gram of support increases along with the amount of immobilized protein, suggesting that the pore size is large enough to avoid mass transfer limitations related to the diffusion of NAD^+/NADH cofactor (much larger molecules than CO_2 and formic acid), as shown in the Figure 6b. Also, the increase in immobilized protein does not affect this aspect. Previous studies reported that the activity decreased as the quantity of immobilized enzyme increased using FDH on natural zeolite (Dp = 13 nm) [22]. In that case, the pore size was probably too narrow, resulting in mass transfer problems due to higher amounts of immobilized protein blocking the cofactor's passage. A major advantage of the synthesis process of this type of mesoporous silica is the possibility to tune the pore size according to the type of enzyme to be immobilized.

3.2.4 Thermal stability

The stability test was carried out only on $MCF_{0.75}$ with an enzymatic load of q = 2 mg_{prot}/g_{supp}. The residual activity (A) of free and immobilized enzyme varied as a function of time, at a temperature of 50 °C (Figure 7). After 24 h of incubation, the free enzyme and immobilized enzyme showed a residual activity of 35% and 75%, respectively. Table 3 reports that the differences between the deactivation constants and the half-life are significantly different. Hence, the obtained stabilization factor (around 3.7) is comparable with those present in the literature. For instance, Binay and colleagues [10] got a F_S of 3.6 for FDH from *Candida methylica* immobilized on Immobead 150 functionalized with aldehyde groups, while Yildirim and co-workers [18] obtained a F_S of 5.3 with FDH from *Candida boidinii* adsorbed

montmorillonite K 10. Covalent immobilization with glyoxyl groups allows achieving very high F_S values, reaching up to 150 in the case of FDH on glyoxyl agarose studied by Bolivar and colleagues [42]. To increase the stability factor and obtain a more stable biocatalyst, the immobilization time could be optimized as observed by Mateo and co-workers with penicillin G acylase [57].

3.2.5 Effect of pH and temperature on FDH activity

The tests to assess the optimal pH and temperature were carried out on free and immobilized FDH on $MCF_{0.75}$. Figure 8a shows a slight decrease in the optimal pH of FDH/$MCF_{0.75}$, from 7.5 (for the free enzyme) to 7. Figure 8b displays no change in the optimum temperature. This observation probably indicates that the conformation of the immobilized enzyme has not changed. However, it should be noted that both the temperature and the pH change in the activity of the immobilized enzyme is less marked than that of the free enzyme, confirming that immobilization makes the enzyme more stable under conditions different from the optimal one.

3.2.6 Reaction of CO_2 reduction and reusability of FDH/$MCF_{0.75}$

The CO_2 reduction reaction was carried out with 1.0 g of FDH/$MCF_{0.75}$ in a sealed glass bottle with [NADH]=10mM in a 0.1 M phosphate buffer and pre-saturated with CO_2. A pH of 7 was used to avoid deactivation of the NADH cofactor, in particular to avoid oxidation at more basic pH and rapid destruction at more acidic pH [58]. The reaction was carried out at room temperature and atmospheric pressure because higher temperatures have the drawback of reducing the CO_2 concentration substantially in aqueous media [59]. The duration was set at 2 h. A concentration of formic acid of 0.08±0.02 mM was obtained, which is very low and it should correspond to a conversion of 0.8% referred to the initial NADH. A similar result was obtained by Alagoz and colleagues using sodium bicarbonate instead of CO_2 for the reduction reaction [30]. Since the reduction reaction is reversible, the formic acid produced is likely converted back into CO_2. The system should be studied more in detail to increase formic acid production and achieve a conversion comparable to free FDH, which is about 30% higher [60].
The results on the reusability of immobilized FDH are shown in Figure 9. After 5 reaction cycles, the residual activity is greater than 70%, which is a value similar to those found in the literature.

Barin and co-workers demonstrated that FDH from *Candida boidinii* immobilized on modified EPSNF retained a residual activity of about 60% after 5 reaction cycles [13]. Furthermore, Binay and colleagues reported that FDH from *Candida methylica* immobilized on modified Immobead 150 kept a residual activity of about 70% after 5 reaction cycles [10].

4. Conclusions

FDH from *Candida boidinii* was covalently immobilized on synthesized mesoporous silica using glyoxyl groups for the first time. Three different types of mesoporous silicas (SBA-15, $MCF_{0.5}$ and $MCF_{0.75}$) were synthesized and used to immobilize the FDH enzyme. The different supports were characterized by FESEM, XRD and N_2 physisorption at -196 °C. In order to bind covalently the enzyme to the different mesoporous silicas, functionalization with glyoxyl groups was performed on the three supports. The immobilized enzyme on the three different supports was characterized in terms of immobilization yield and specific activity. The highest specific activity (1.05 UI $g_{supp.}^{-1}$) was achieved with the FDH/$MCF_{0.75}$, with an immobilization yield of 52.2%. The enzyme immobilization was also verified by optical fluorescence microscopy after the effective dye fluorescence labelling of the enzyme. The yield of immobilization obtained was not very high and most likely by increasing the immobilization times by a few hours it can be boosted up to 100%. However, longer times at the immobilization pH (10.05) could inactivate the enzyme. Thus, another strategy to increase the immobilization yield may be the use of heterofunctional supports, such as amino-glyoxyl silicas. In this form, the enzyme is first immobilized by ionic interactions, which occurs at neutral pH, and then the covalent bond is formed in a short-time reaction at basic pH. Using $MCF_{0.75}$ as support, the immobilization yield and the specific activity vary as the enzymatic load varies. The thermal stability at 50 °C was evaluated and, with FDH/$MCF_{0.75}$, an F_S=4 was reached. Finally, the residual activity of 70% was achieved after 5 cycles of reuse.

The studied biocatalyst turned out to be really promising since it can be used for CO_2 reduction to produce high value-added molecules such as formic acid or, in enzyme-catalyzed cascade reactions, methanol. However, future work should include a smart optimization of the system since it needs further improvement to be exploited in industrial applications. Furthermore, this immobilization technique and the synthesized MCF supports are versatile, and the pore diameter could be finely tuned to immobilize even different enzymes.

Declaration of interest

The authors declare no competing interests.

Acknowledgement

The authors thank the project “VALPO4CIRCULAR ECONOMY” funded by Compagnia San Paolo and Politecnico di Torino and FONDECYT grant number 11180967 for the financial support and the internationalization of the research.

References

[1] L. Fraccascia, I. Giannoccaro, Analyzing CO_2 emissions flows in the world economy using Global Emission Chains and Global Emission Trees, J. Clean. Prod. 234 (2019) 1399–1420. https://doi.org/10.1016/j.jclepro.2019.06.297.

[2] H. Choe, J.C. Joo, D.H. Cho, M.H. Kim, S.H. Lee, K.D. Jung, Y.H. Kim, Efficient CO_2-reducing activity of NAD-dependent formate dehydrogenase from *Thiobacillus* sp. KNK65MA for formate production from CO_2 gas, PLoS One. 9 (2014). https://doi.org/10.1371/journal.pone.0103111.

[3] N. Long, J. Lee, K.-K. Koo, P. Luis, M. Lee, Recent Progress and Novel Applications in Enzymatic Conversion of Carbon Dioxide, Energies. 10 (2017) 473. https://doi.org/10.3390/en10040473.

[4] Y. Amao, Formate dehydrogenase for CO_2 utilization and its application, J. CO_2 Util. 26 (2018) 623–641. https://doi.org/10.1016/j.jcou.2018.06.022.

[5] Y.K. Kim, S.Y. Lee, B.K. Oh, Enhancement of formic acid production from CO_2 in formate dehydrogenase reaction using nanoparticles, RSC Adv. 6 (2016) 109978–109982.

https://doi.org/10.1039/c6ra23793b.

[6] A. Dibenedetto, P. Stufano, W. Macyk, T. Baran, C. Fragale, M. Costa, M. Aresta, Hybrid technologies for an enhanced carbon recycling based on the enzymatic reduction of CO_2 to methanol in water: Chemical and photochemical NADH regeneration, ChemSusChem. 5 (2012) 373–378. https://doi.org/10.1002/cssc.201100484.

[7] S.W. Xu, Y. Lu, J. Li, Z.Y. Jiang, H. Wu, Efficient conversion of CO_2 to methanol catalyzed by three dehydrogenases co-encapsulated in an alginate-silica (ALG-SiO_2) hybrid gel, Ind. Eng. Chem. Res. 45 (2006) 4567–4573. https://doi.org/10.1021/ie051407l.

[8] R. Obert, B.C. Dave, Enzymatic Conversion of Carbon Dioxide to Methanol: Enhanced Methanol Production in Silica Sol-Gel Matrices, Ind. Eng. Chem. Res. 37 (1998) 12192–12193. https://doi.org/10.1021/ja991899r.

[9] M. Zezzi do Valle Gomes, A.E.C. Palmqvist, Immobilization of formaldehyde dehydrogenase in tailored siliceous mesostructured cellular foams and evaluation of its activity for conversion of formate to formaldehyde, Colloids Surfaces B Biointerfaces. 163 (2018) 41–46. https://doi.org/10.1016/j.colsurfb.2017.11.069.

[10] B. Binay, D. Alagöz, D. Yildirim, A. Çelik, S. Seyhan Tükel, Highly stable and reusable immobilized formate dehydrogenases: Promising biocatalysts for in situ regeneration of NADH, Beilstein J. Org. Chem. 12 (2016) 271–277. https://doi.org/10.3762/bjoc.12.29.

[11] J. Begemann, R.B.H. Ohs, A.B. Ogolong, W. Eberhard, M.B. Ansorge-Schumacher, A.C. Spiess, Model-based analysis of a reactor and control concept for oxidoreductions based on exhaust CO_2-measurement, Process Biochem. 51 (2016) 1397–1405. https://doi.org/10.1016/j.procbio.2016.06.024.

[12] R. Barin, D. Biria, S. Rashid-Nadimi, M.A. Asadollahi, Investigating the enzymatic CO_2 reduction to formate with electrochemical NADH regeneration in batch and semi-

continuous operations, Chem. Eng. Process. - Process Intensif. 140 (2019) 78–84. https://doi.org/10.1016/j.cep.2019.04.020.

[13] R. Barin, D. Biria, S. Rashid-Nadimi, M.A. Asadollahi, Enzymatic CO_2 reduction to formate by formate dehydrogenase from *Candida boidinii* coupling with direct electrochemical regeneration of NADH, J. CO_2 Util. 28 (2018) 117–125. https://doi.org/10.1016/j.jcou.2018.09.020.

[14] L. Zhang, J. Liu, J. Ong, S.F.Y. Li, Specific and sustainable bioelectro-reduction of carbon dioxide to formate on a novel enzymatic cathode, Chemosphere. 162 (2016) 228–234. https://doi.org/10.1016/j.chemosphere.2016.07.102.

[15] S. Sultana, P. Chandra Sahoo, S. Martha, K. Parida, A review of harvesting clean fuels from enzymatic CO_2 reduction, RSC Adv. 6 (2016) 44170–44194. https://doi.org/10.1039/c6ra05472b.

[16] F. Marpani, M. Pinelo, A.S. Meyer, Enzymatic conversion of CO_2 to CH_3OH via reverse dehydrogenase cascade biocatalysis: Quantitative comparison of efficiencies of immobilized enzyme systems, Biochem. Eng. J. 127 (2017) 217–228. https://doi.org/10.1016/j.bej.2017.08.011.

[17] A. Illanes, Enzyme biocatalysis: Principles and applications, Springer, 2008. https://doi.org/10.1007/978-1-4020-8361-7.

[18] D. Yildirim, D. Alagöz, A. Toprak, S. Tükel, R. Fernandez-Lafuente, Tuning dimeric formate dehydrogenases reduction/oxidation activities by immobilization, Process Biochem. 85 (2019) 97–105. https://doi.org/10.1016/j.procbio.2019.07.001.

[19] X. Wang, Z. Li, J. Shi, H. Wu, Z. Jiang, W. Zhang, X. Song, Q. Ai, Bioinspired approach to multienzyme cascade system construction for efficient carbon dioxide reduction, ACS Catal. 4 (2014) 962–972. https://doi.org/10.1021/cs401096c.

[20] C. Bernal, L. Sierra, M. Mesa, Improvement of thermal stability of β-galactosidase from *Bacillus circulans* by multipoint covalent immobilization in hierarchical macro-mesoporous silica, J. Mol. Catal. B Enzym. 84 (2012) 166–172. https://doi.org/10.1016/j.molcatb.2012.05.023.

[21] C. Bernal, P. Urrutia, A. Illanes, L. Wilson, Hierarchical meso-macroporous silica grafted with glyoxyl groups: Opportunities for covalent immobilization of enzymes, N. Biotechnol. 30 (2013) 500–506. https://doi.org/10.1016/j.nbt.2013.01.011.

[22] G. Pietricola, C. Ottone, D. Fino, T. Tommasi, Enzymatic reduction of CO_2 to formic acid using FDH immobilized on natural zeolite, J. CO_2 Util. 42 (2020) 101343. https://doi.org/10.1016/j.jcou.2020.101343.

[23] N. Balistreri, D. Gaboriau, C. Jolivalt, F. Launay, Covalent immobilization of glucose oxidase on mesocellular silica foams: Characterization and stability towards temperature and organic solvents, J. Mol. Catal. B Enzym. 127 (2016) 26–33. https://doi.org/10.1016/j.molcatb.2016.02.003.

[24] K. Kannan, R.V. Jasra, Immobilization of alkaline serine endopeptidase from *Bacillus licheniformis* on SBA-15 and MCF by surface covalent binding, J. Mol. Catal. B Enzym. 56 (2009) 34–40. https://doi.org/10.1016/j.molcatb.2008.04.007.

[25] J. Sun, D. Zhang, W. Zhao, Q. Ji, K. Ariga, Enhanced Activity of Alcohol Dehydrogenase in Porous Silica Nanosheets with Wide Size Distributed Mesopores, Bull. Chem. Soc. Jpn. 92 (2019) 275–282. https://doi.org/10.1246/bcsj.20180201.

[26] M. Dreifke, F.J. Brieler, M. Fröba, Immobilization of Alcohol Dehydrogenase from *E. coli* onto Mesoporous Silica for Application as a Cofactor Recycling System, ChemCatChem. 9 (2017) 1197–1210. https://doi.org/10.1002/cctc.201601288.

[27] P.S. Nabavi Zadeh, M. Zezzi Do Valle Gomes, B. Åkerman, A.E.C. Palmqvist, Förster

Resonance Energy Transfer Study of the Improved Biocatalytic Conversion of CO_2 to Formaldehyde by Coimmobilization of Enzymes in Siliceous Mesostructured Cellular Foams, ACS Catal. 8 (2018) 7251–7260. https://doi.org/10.1021/acscatal.8b01806.

[28] J.S. Lettow, Y.J. Han, P. Schmidt-Winkel, P. Yang, D. Zhao, G.D. Stucky, J.Y. Ying, Hexagonal to mesocellular foam phase transition in polymer-templated mesoporous silicas, Langmuir. 16 (2000) 8291–8295. https://doi.org/10.1021/la000660h.

[29] N. Kharrat, Y. Ben Ali, S. Marzouk, Y.T. Gargouri, M. Karra-Châabouni, Immobilization of Rhizopus oryzae lipase on silica aerogels by adsorption: Comparison with the free enzyme, Process Biochem. 46 (2011) 1083–1089. https://doi.org/10.1016/j.procbio.2011.01.029.

[30] D. Alagöz, A. Çelik, D. YIldIrIm, S.S. Tükel, B. Binay, Covalent immobilization of Candida methylica formate dehydrogenase on short spacer arm aldehyde group containing supports, J. Mol. Catal. B Enzym. 130 (2016) 40–47. https://doi.org/10.1016/j.molcatb.2016.05.005.

[31] M. Piumetti, M. Hussain, D. Fino, N. Russo, Mesoporous silica supported Rh catalysts for high concentration N_2O decomposition, Appl. Catal. B Environ. 165 (2015) 158–168. https://doi.org/10.1016/j.apcatb.2014.10.008.

[32] M. Piumetti, B. Bonelli, P. Massiani, S. Dzwigaj, I. Rossetti, S. Casale, L. Gaberova, M. Armandi, E. Garrone, Effect of vanadium dispersion and support properties on the catalytic activity of V-SBA-15 and V-MCF mesoporous materials prepared by direct synthesis, in: Catal. Today, Elsevier, 2011: pp. 458–464. https://doi.org/10.1016/j.cattod.2010.10.066.

[33] H. Kim, J.C. Jung, S.H. Yeom, K.Y. Lee, J. Yi, I.K. Song, Immobilization of a heteropolyacid catalyst on the aminopropyl-functionalized mesostructured cellular foam

(MCF) silica, Mater. Res. Bull. 42 (2007) 2132–2142. https://doi.org/10.1016/j.materresbull.2007.01.010.

[34] A. Karkamkar, S.S. Kim, T.J. Pinnavaia, Hydrothermal restructuring of the cell and window sizes of silica foams, Chem. Mater. 15 (2003) 11–13. https://doi.org/10.1021/cm020867r.

[35] Y. Su, Y.M. Liu, L.C. Wang, M. Chen, Y. Cao, W.L. Dai, H.Y. He, K.N. Fan, Tungsten-containing MCF silica as active and recyclable catalysts for liquid-phase oxidation of 1,3-butanediol to 4-hydroxy-2-butanone, Appl. Catal. A Gen. 315 (2006) 91–100. https://doi.org/10.1016/j.apcata.2006.09.002.

[36] W.W. Lukens, P. Schmidt-Winkel, D. Zhao, J. Feng, G.D. Stucky, Evaluating pore sizes in mesoporous materials: a simplified standard adsorption method and a simplified Broekhoff-de Boer method, Langmuir. 15 (1999) 5403–5409. https://doi.org/10.1021/la990209u.

[37] P. Vejayakumaran, I.A. Rahman, C.S. Sipaut, J. Ismail, C.K. Chee, Structural and thermal characterizations of silica nanoparticles grafted with pendant maleimide and epoxide groups, J. Colloid Interface Sci. 328 (2008) 81–91. https://doi.org/10.1016/j.jcis.2008.08.054.

[38] A.H. Orrego, M. Romero-Fernández, M. Del, C. Millán-Linares, J. Pedroche, J.M. Guisán, J. Rocha-Martin, High Stabilization of Enzymes Immobilized on Rigid Hydrophobic Glyoxyl-Supports: Generation of Hydrophilic Environments on Support Surfaces, Catalysts. 10 (2020). https://doi.org/10.3390/catal10060676.

[39] J.M. Guisán, Aldehyde-agarose gels as activated supports for immobilization-stabilization of enzymes, Enzyme Microb. Technol. 10 (1988) 375–382. https://doi.org/10.1016/0141-0229(88)90018-X.

[40] J.M. Bolivar, L. Wilson, S.A. Ferrarotti, R. Fernandez-Lafuente, J.M. Guisan, C. Mateo, Stabilization of a formate dehydrogenase by covalent immobilization on highly activated glyoxyl-agarose supports, Biomacromolecules. 7 (2006) 669–673. https://doi.org/10.1021/bm050947z.

[41] H.P. Erickson, Size and shape of protein molecules at the nanometer level determined by sedimentation, gel filtration, and electron microscopy, Biol. Proced. Online. 11 (2009) 32–51. https://doi.org/10.1007/s12575-009-9008-x.

[42] J.M. Bolivar, L. Wilson, S.A. Ferrarotti, R. Fernandez-Lafuente, J.M. Guisan, C. Mateo, Evaluation of different immobilization strategies to prepare an industrial biocatalyst of formate dehydrogenase from *Candida Boidinii*, Enzyme Microb. Technol. 40 (2007) 540–546. https://doi.org/10.1016/j.enzmictec.2006.05.009.

[43] M.M. Bradford, A rapid and sensitive method for the quantitation of microgram quantities of protein utilizing the principle of protein-dye binding, Anal. Biochem. 72 (1976) 248–254. https://doi.org/10.1016/0003-2697(76)90527-3.

[44] J.M. Guisan, J.M. Bolivar, F. López-Gallego, J. Rocha-Martín, eds., Immobilization of Enzymes and Cells, Springer US, New York, NY, 2020. https://doi.org/10.1007/978-1-0716-0215-7.

[45] S. Velasco-Lozano, A.I. Benítez-Mateos, F. López-Gallego, Co-immobilized Phosphorylated Cofactors and Enzymes as Self-Sufficient Heterogeneous Biocatalysts for Chemical Processes, Angew. Chemie - Int. Ed. 56 (2017) 771–775. https://doi.org/10.1002/anie.201609758.

[46] M. Kruk, M. Jaroniec, C.H. Ko, R. Ryoo, Characterization of the porous structure of SBA-15, Chem. Mater. 12 (2000) 1961–1968. https://doi.org/10.1021/cm000164e.

[47] C.Y. Chen, H.X. Li, M.E. Davis, Studies on mesoporous materials. I. Synthesis and

characterization of MCM-41, Microporous Mater. 2 (1993) 17–26. https://doi.org/10.1016/0927-6513(93)80058-3.

[48] T. Tsoncheva, L. Ivanova, J. Rosenholm, M. Linden, Cobalt oxide species supported on SBA-15, KIT-5 and KIT-6 mesoporous silicas for ethyl acetate total oxidation, Appl. Catal. B Environ. 89 (2009) 365–374. https://doi.org/10.1016/j.apcatb.2008.12.015.

[49] U. Ciesla, F. Schüth, Ordered mesoporous materials, Microporous Mesoporous Mater. 27 (1999) 131–149. https://doi.org/10.1016/S1387-1811(98)00249-2.

[50] M. Piumetti, B. Bonelli, P. Massiani, Y. Millot, S. Dzwigaj, L. Gaberova, M. Armandi, E. Garrone, Novel vanadium-containing mesocellular foams (V-MCF) obtained by direct synthesis, Microporous Mesoporous Mater. 142 (2011) 45–54. https://doi.org/10.1016/j.micromeso.2010.11.010.

[51] S. Brunauer, L.S. Deming, W.E. Deming, E. Teller, On a Theory of the van der Waals Adsorption of Gases, J. Am. Chem. Soc. 62 (1940) 1723–1732. https://doi.org/10.1021/ja01864a025.

[52] E.M. Johansson, Controlling the Pore Size and Morphology of Mesoporous Silica, 2010.

[53] J. Rouquerol, F. Rouquerol, P. Llewellyn, G. Maurin, K.S.W. Sing, Adsorption by Powders and Porous Solids: Principles, Methodology and Applications: Second Edition, 2013. https://doi.org/10.1016/C2010-0-66232-8.

[54] A. Sayari, Y. Yang, M. Kruk, M. Jaroniec, Expanding the pore size of MCM-41 silicas: Use of amines as expanders in direct synthesis and postsynthesis procedures, J. Phys. Chem. B. 103 (1999) 3651–3658. https://doi.org/10.1021/jp984504j.

[55] M. Piumetti, B. Bonelli, M. Armandi, L. Gaberova, S. Casale, P. Massiani, E. Garrone, Vanadium-containing SBA-15 systems prepared by direct synthesis: Physico-chemical and catalytic properties in the decomposition of dichloromethane, Microporous

Mesoporous Mater. 133 (2010) 36–44. https://doi.org/10.1016/j.micromeso.2010.04.011.

[56] H. Schutte, J. Flossdorf, H. Sahm, M.-R. Kula, Purification and Properties of Formaldehyde Dehydrogenase and Formate Dehydrogenase from *Candida boidinii*, Eur. J. Biochem. 62 (1976) 151–160. https://doi.org/10.1111/j.1432-1033.1976.tb10108.x.

[57] C. Mateo, O. Abian, R. Fernandez-Lafuente, J.M. Guisan, Increase in conformational stability of enzymes immobilized on epoxy-activated supports by favoring additional multipoint covalent attachment, Enzyme Microb. Technol. 26 (2000) 509–515. https://doi.org/10.1016/S0141-0229(99)00188-X.

[58] O.H. Lowry, J. V. Passonneau, M.K. Rock, The stability of pyridine nucleotides., J. Biol. Chem. 236 (1961) 2756–2759.

[59] R.H. Perry, D.W. Green, Perry's Chemical Engineers' Handbook, 8th Edition, McGraw-Hill, 2007.

[60] S. Kim, M.K. Kim, S.H. Lee, S. Yoon, K.D. Jung, Conversion of CO_2 to formate in an electroenzymatic cell using *Candida boidinii* formate dehydrogenase, J. Mol. Catal. B Enzym. 102 (2014) 9–15. https://doi.org/10.1016/j.molcatb.2014.01.007.

Table 1 Textural properties of the prepared materials derived from the N_2 physisorption at -196 °C.

Sample	S_{BET} (m^2 g^{-1})[a]	V_p (cm^3 g^{-1})[b]	V_{micro} (cm^3 g^{-1})[c]	D_p (nm)
SBA-15	674	0.71	$4.34 \cdot 10^{-2}$	4 [d]
$MCF_{0.5}$	573	0.91	$3.93 \cdot 10^{-2}$	20 [e]
$MCF_{0.75}$	600	1.40	$4.43 \cdot 10^{-2}$	25 [e]

[a] Surface area derived by the BET method.
[b] Pore volume evaluated by the BJH method, during the desorption phase.
[c] Micropore volume.
[d] Average pore diameter evaluated by the BJH method, during the desorption phase.
[e] Cell diameter determined from adsorption branches of the N_2 isotherms (BdB–FHH method).

Table 2 - Specific activities and immobilization yields for the FDH over different supports. Different letters (x,y and z) indicate significant differences ($P < 0.05$, Tukey HSD) in IY and specific activities of immobilized FDH between different supports.

Sample	D_p(nm)[a]	$A_{g\ supp.}$ (µmol min^{-1} $g_{supp.}^{-1}$)[b]	$A_{mg\ imm.prot.}$ (µmol min^{-1} $mg_{imm.prot.}^{-1}$)[c]	IY (%)
FDH/SBA-15	4	0.37 ± 0.05 z	0.63 ± 0.02 y	29.3 ± 4.3 z
FDH/$MCF_{0.5}$	20	0.75 ± 0.06 y	0.54 ± 0.01 z	69.4 ± 6.1 x
FDH/$MCF_{0.75}$	25	1.05 ± 0.05 x	1.01 ± 0.02 x	52.2 ± 3.6 y

[a] Average pore diameter evaluated by the BJH method, during the desorption phase.
[b] Specific activity of FDH reffered to g of support.
[c] Specific activity of FDH reffered to mg of immobilized enzyme.

Table 3 Deactivation constant (k_D), half-life ($t_{1/2}$) and stabilization factor (F_s) obtained from the first-order deactivation model with no residual activity. Different letters (x,y) indicate significant differences ($P < 0.05$, Tukey HSD) in k_D and $t_{1/2}$ between free and immobilized enzyme.

Sample	k_D (h^{-1})	$t_{1/2}$ (h)	F_S	R^2
Free FDH	0.052 ± 0.006 x	13.6 ± 1.6 y	-	0.99
FDH/MCF$_{0.75}$	0.014 ± 0.002 y	50.2.0 ± 5.91 x	3.69	0.93

Figure 1. Conversion of CO_2 to methanol using three enzymes in cascade

Figure 2. XRD pattern of the SBA-15-type support.

Figure 3. N_2 sorption isotherms for SBA-15 (a), $MCF_{0.5}$ (b) and $MCF_{0.75}$ (c) materials.

Figure 4. FESEM images of the supports: A) SBA-15, B) $MCF_{0.5}$ and C) $MCF_{0.75}$.

Figure 5. Optical fluorescence microscopy images of the FITC-labelled (a-b) FDH/$MCF_{0.75}$ sample and (c-d) $MCF_{0.75}$. Images (a) and (c) are in brightfiels, showing the silica particles on the glass slides, while images (b) and (d) depicts the green channel, showing the fluorescence emitted by the FITC dye.

Figure 6. a) Immobilization yield (IY) as a function of mg of enzyme offered (q_{off}). b) Specific activity (A) as a function of effective mg of enzyme loaded (q_{eff}).

Figure 7. Residual activity of free and immobilized enzyme incubated at 50°C.

Figure 8. Optimum pH (a) and T (b) for FDH immobilized on $MCF_{0.75}$ and free FDH.

Figure 9. Reusability test of FDH/$MCF_{0.75}$

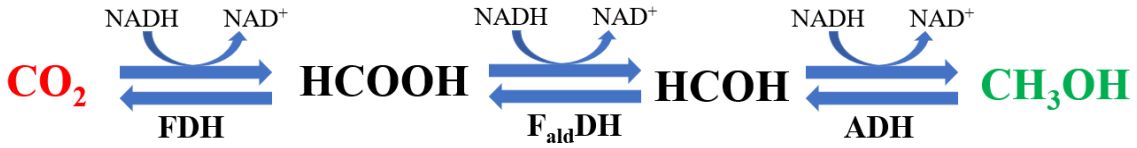
NADH
NAD+
CO2
FDH
HCOOH
NADH
NAD+
Fald DH
HCOH
NADH
NAD+
ADH
CH3OH

Figure 1.

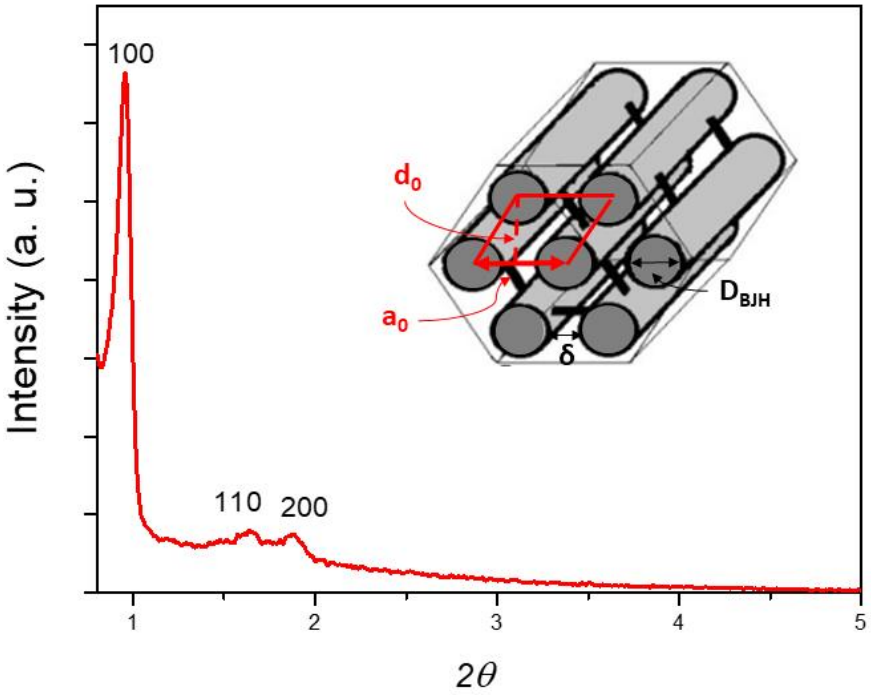

Figure 2.

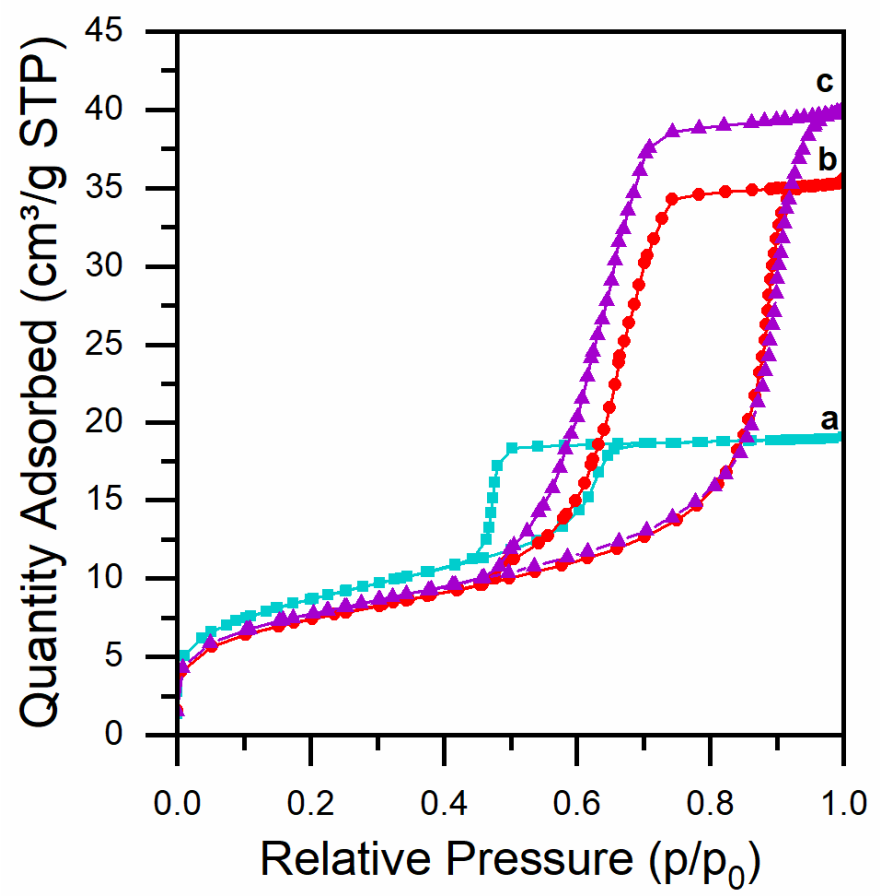
Quantity Adsorbed (cm³/g STP)
Relative Pressure (p/p0)
0
5
10
15
20
25
30
35
40
45
0.0
0.2
0.4
0.6
0.8
1.0
a
b
c

Figure 3.

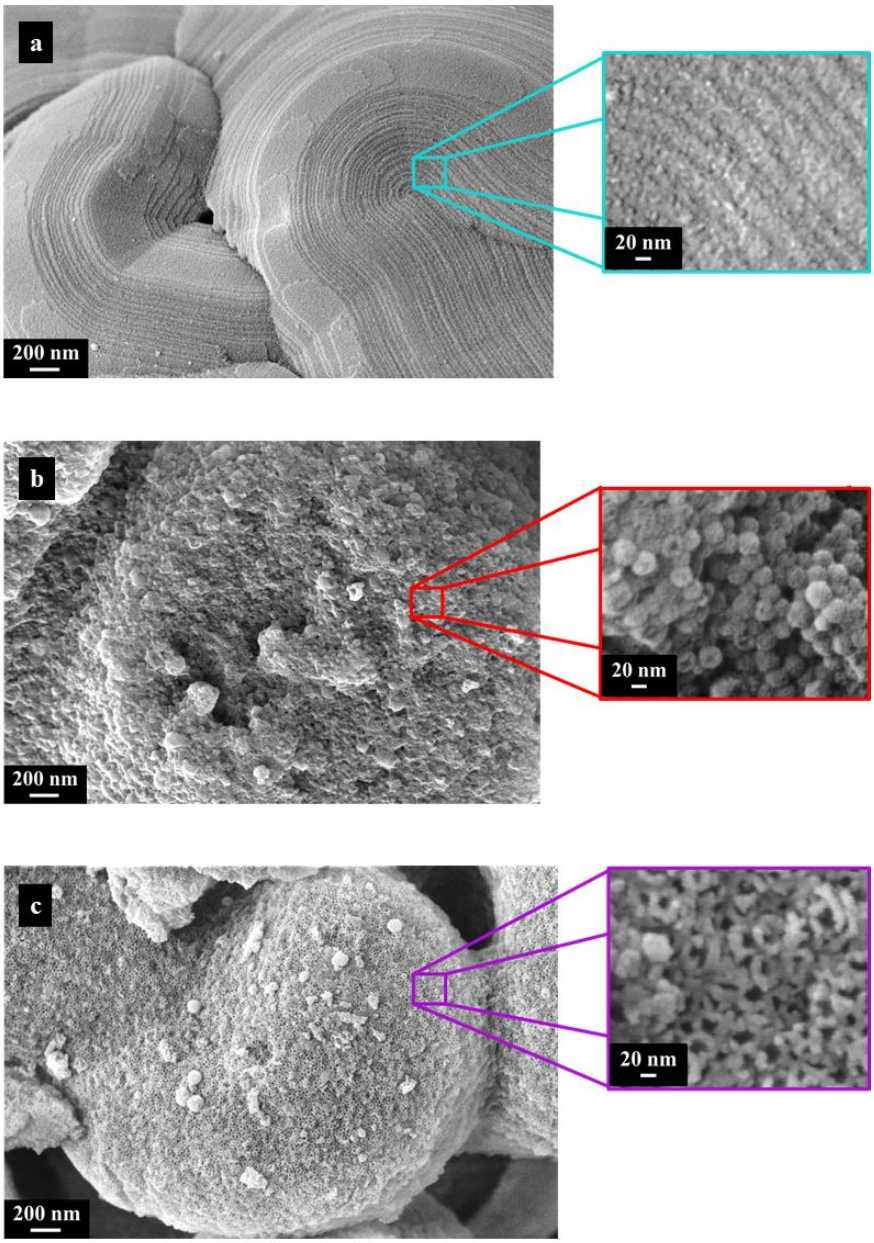

Figure 4.

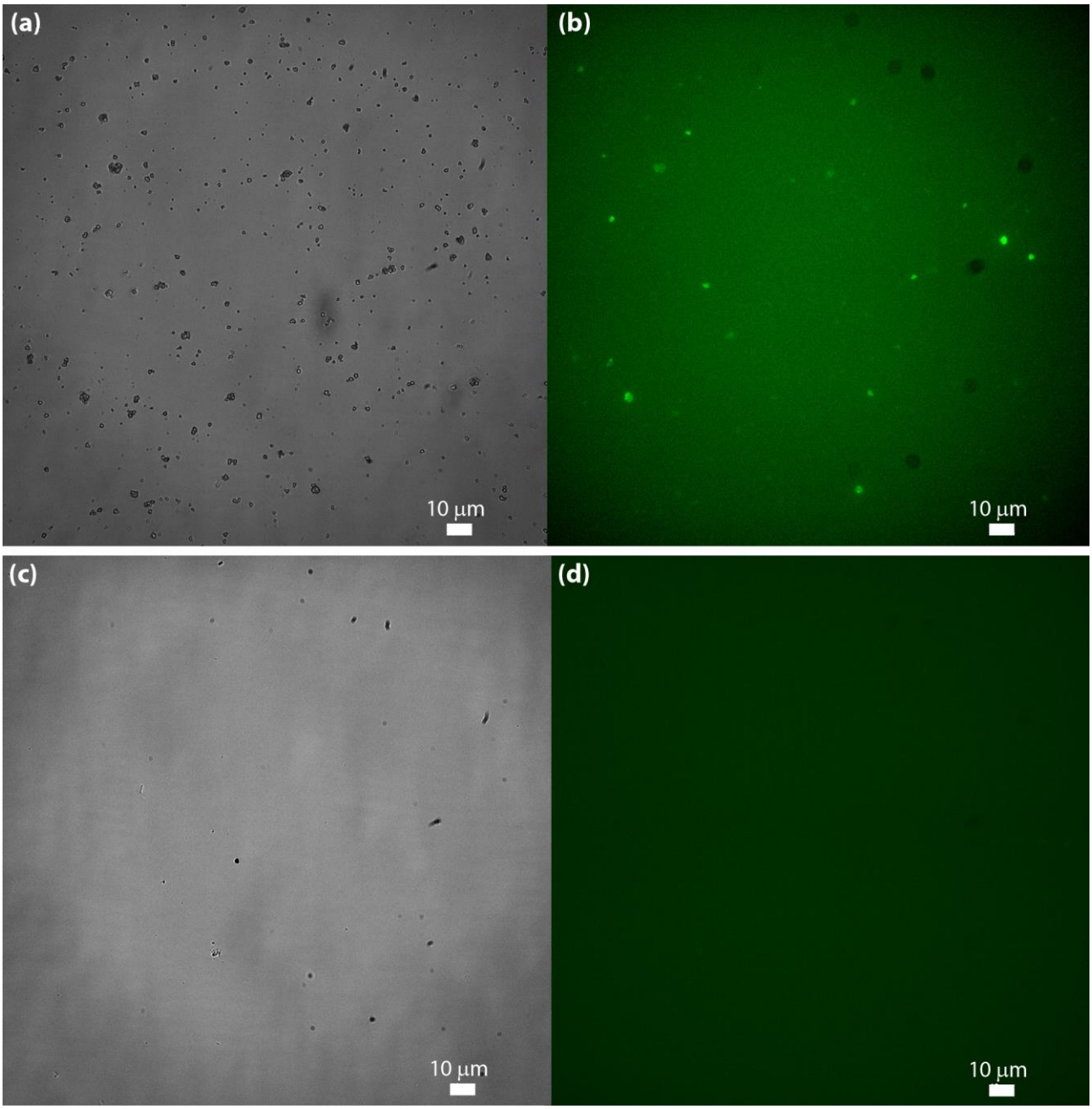

Figure 5.

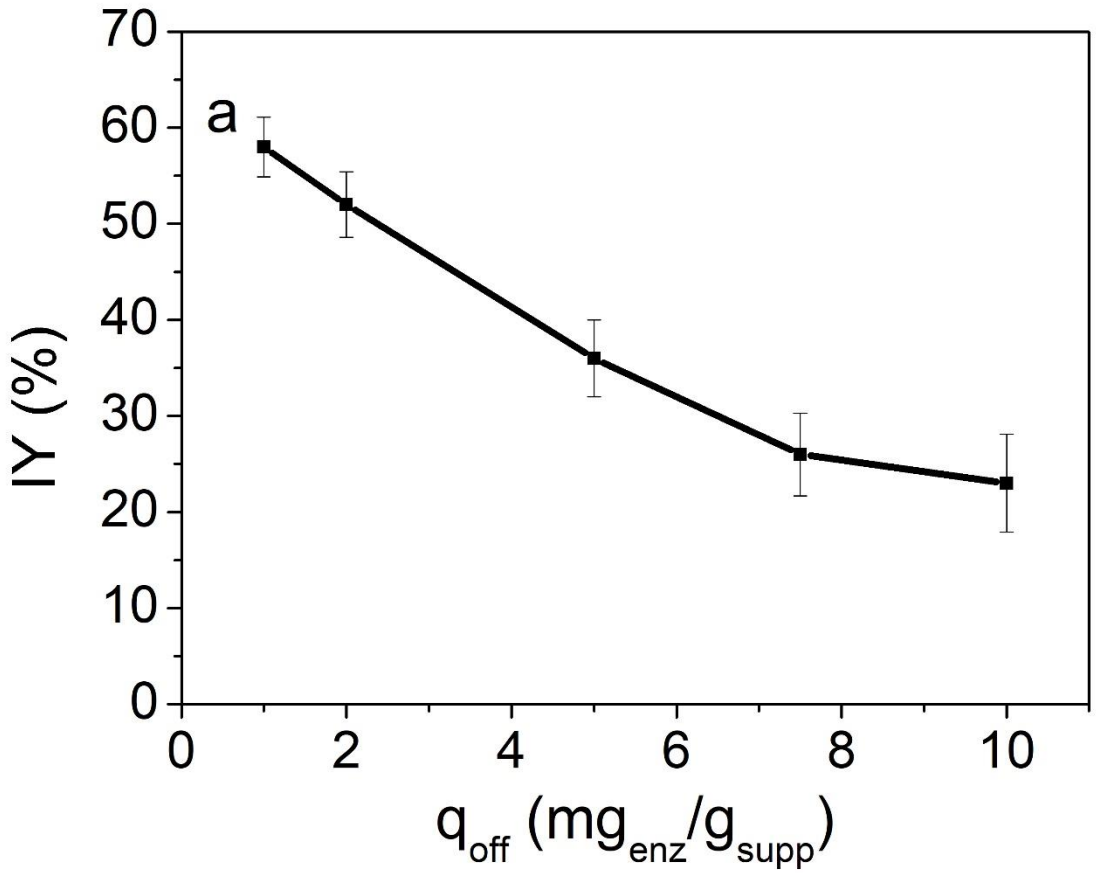
a
IY (%)
70
60
50
40
30
20
10
0
0
2
4
6
8
10
q_{off} (mg_{enz}/g_{supp})

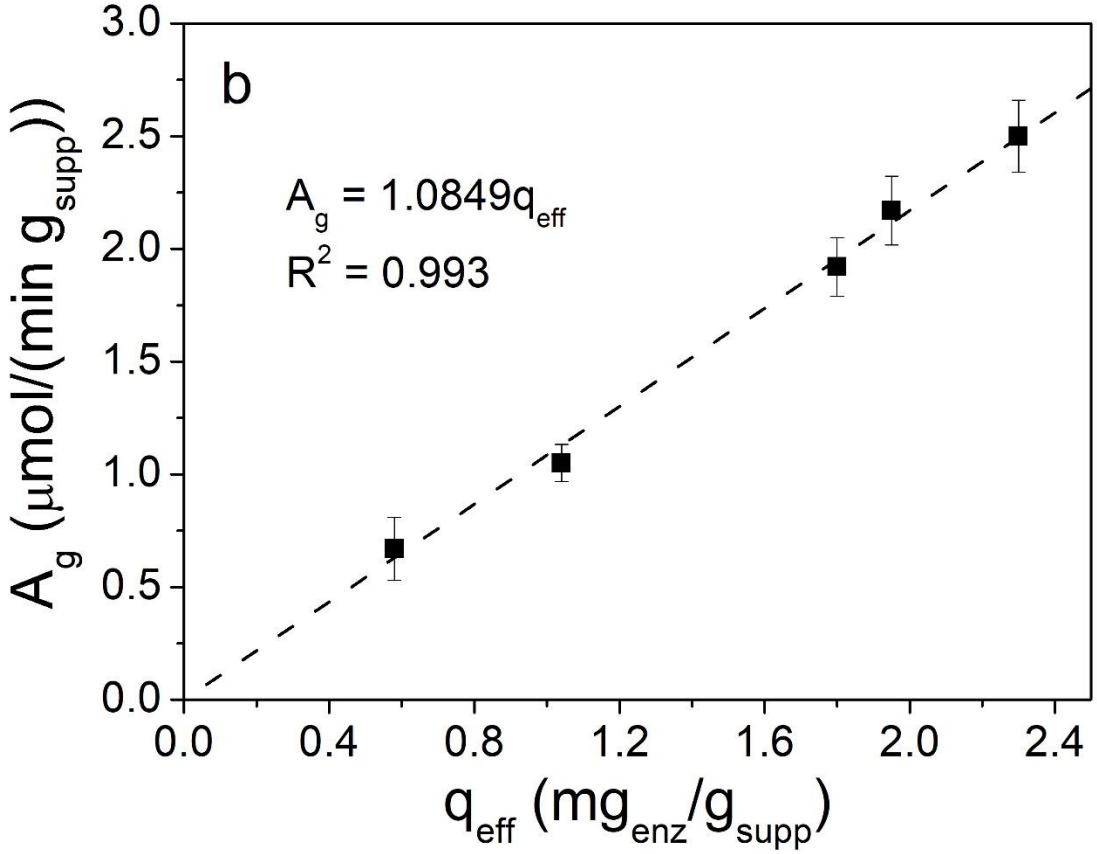
b
$A_g = 1.0849q_{eff}$
$R^2 = 0.993$
A_g (µmol/(min g_{supp}))
q_{eff} (mg_{enz}/g_{supp})
0.0
0.5
1.0
1.5
2.0
2.5
3.0
0.0
0.4
0.8
1.2
1.6
2.0
2.4

Figure 6.

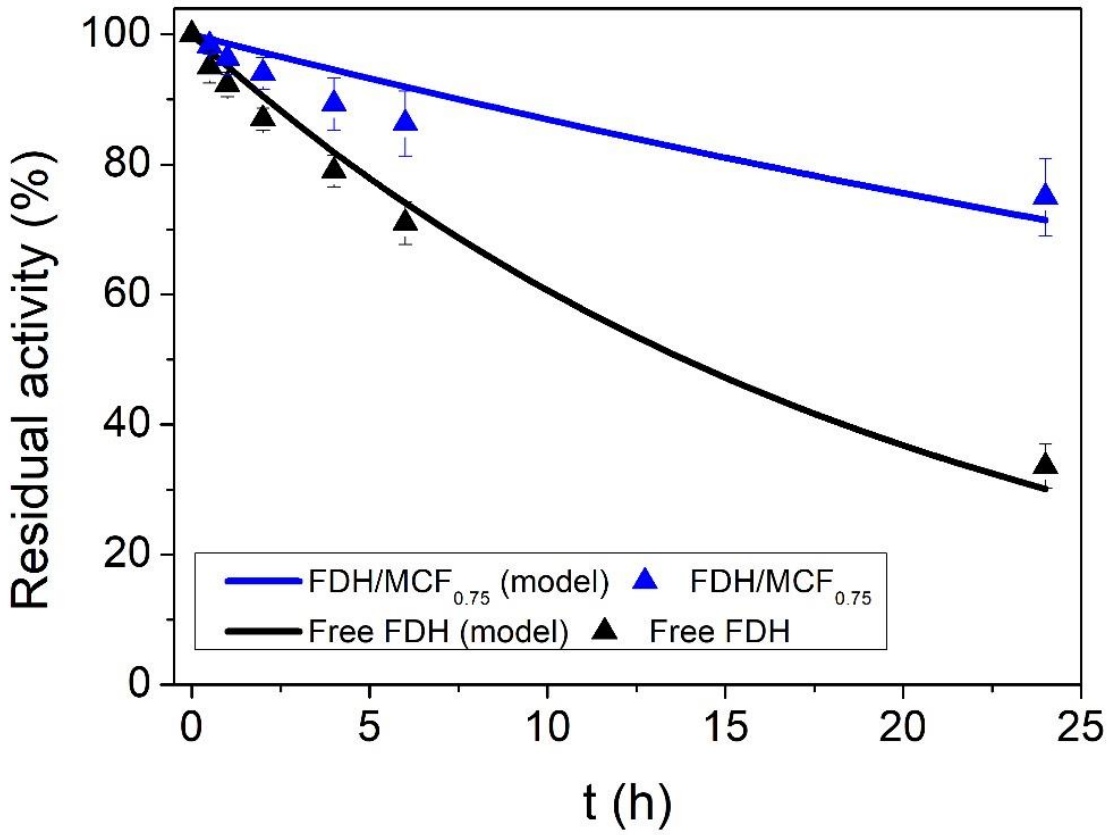
Residual activity (%)
100
80
60
40
20
0
0
5
10
15
20
25
t (h)
FDH/MCF0.75 (model)
FDH/MCF0.75
Free FDH (model)
Free FDH

Figure 7.

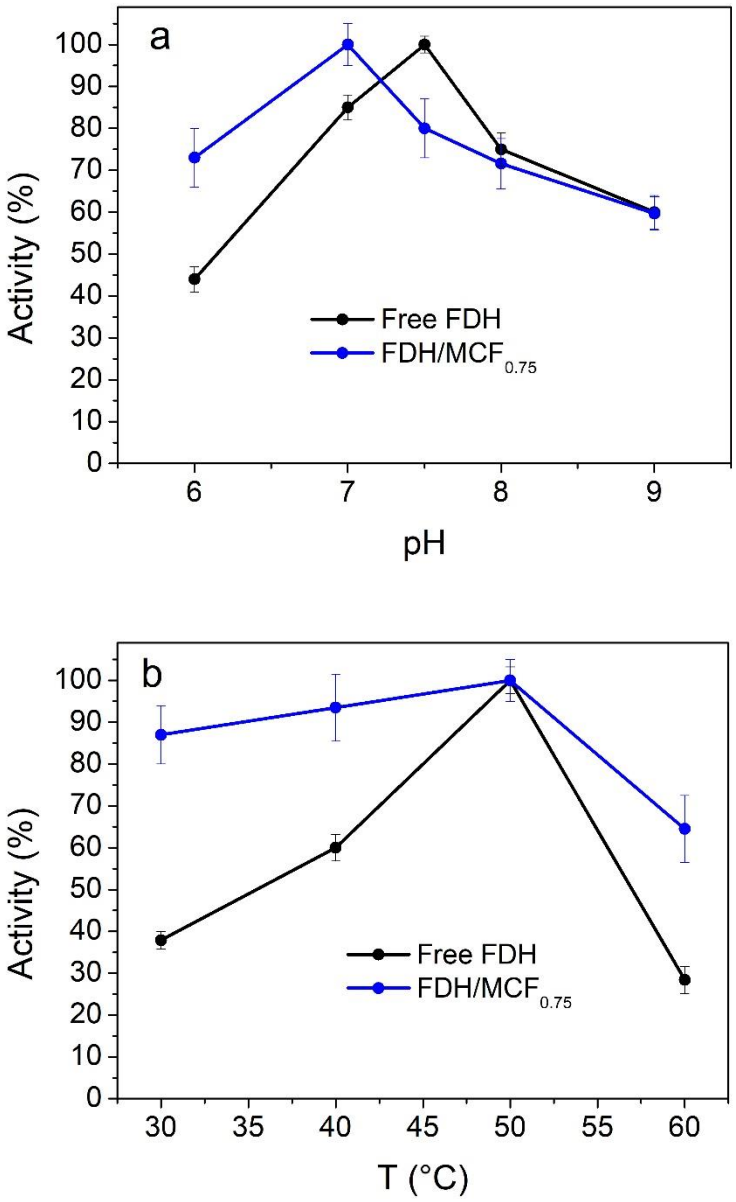
a
Activity (%)
pH
Free FDH
FDH/MCF0.75
b
Activity (%)
T (°C)
Free FDH
FDH/MCF0.75

Figure 8.

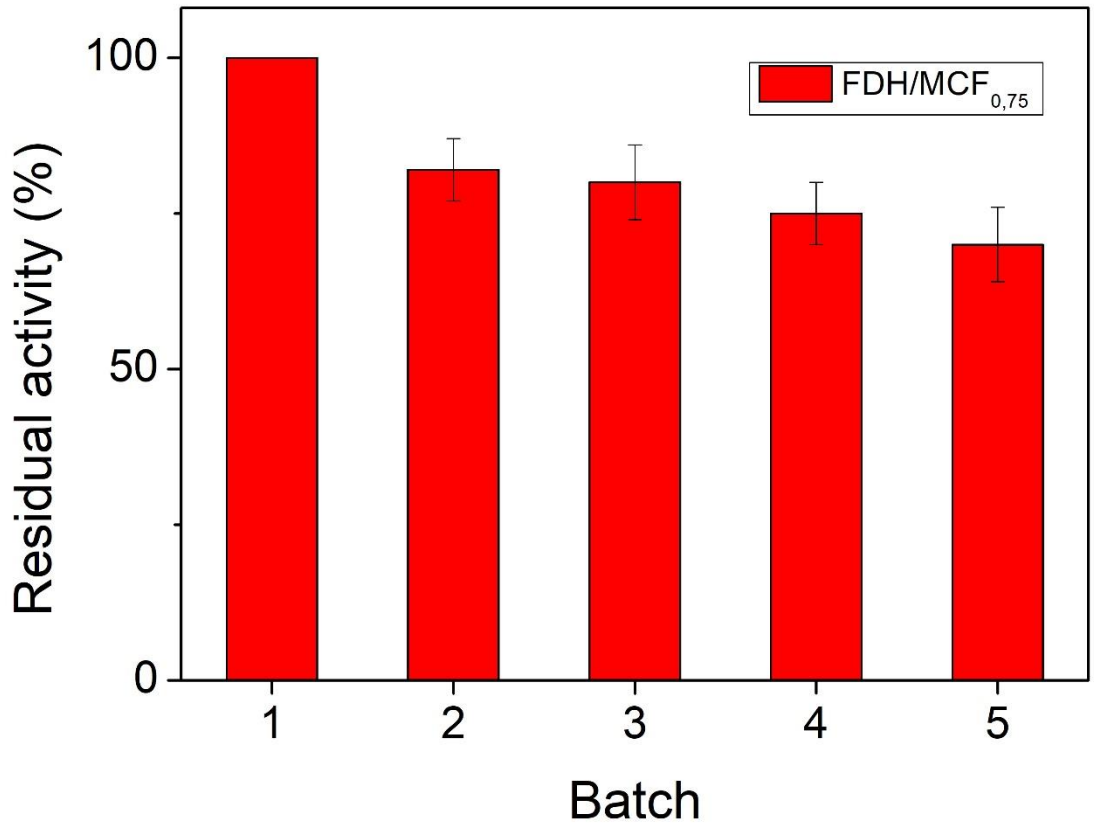

Figure 9.